

Square Grid Benchmarks for *Source-Terminal* Network Reliability Estimation*

Roger Paredes[†] Leonardo Duenas-Osorio

Rice University, Houston TX, USA.
03/2018

This document describes a synthetic benchmark data set that can be used to compare network reliability estimation methods [1, 2]. The document is structured as follows: Section 1 introduces the *source-terminal* network reliability problem and an input file format used to encode instances of the problem. Section 2 provides details on the set of benchmarks we consider and the setup for numerical experiments. Section 3 gives reference computations via exact bounds and crude Monte Carlo simulation estimates. Section 4 concludes this benchmarking study.

1 Introduction

The *source-terminal* network reliability problem we consider is defined as follows. Given an undirected graph $G(V, E)$, where V is the set of nodes and E is the set of links, the *source-terminal* network reliability problem asks to compute the probability that nodes $s, t \in V$ remain connected, here denoted $r_{s,t}$, given that every link $e \in E$ fails with known probability p_e .

Physical networks studied in practice tend to be highly reliable, thus the real challenge is that of knowing the failure probability of the network (or unreliability), herein denoted $u_{s,t}$. In the exact estimation setting $u_{s,t} = 1 - r_{s,t}$. However, in the approximation setting we focus on computing $\hat{u}_{s,t}$ directly with small relative error $|\hat{u}_{s,t} - u_{s,t}|/u_{s,t}$, otherwise an estimate of $r_{s,t}$ when $r_{s,t} \approx 1$ would give a poor estimate of $u_{s,t}$ in terms of relative error.

*cite as Paredes and Duenas-Osorio [1] or Paredes et al. [2].

[†]roger.paredes(at)rice(dot)edu

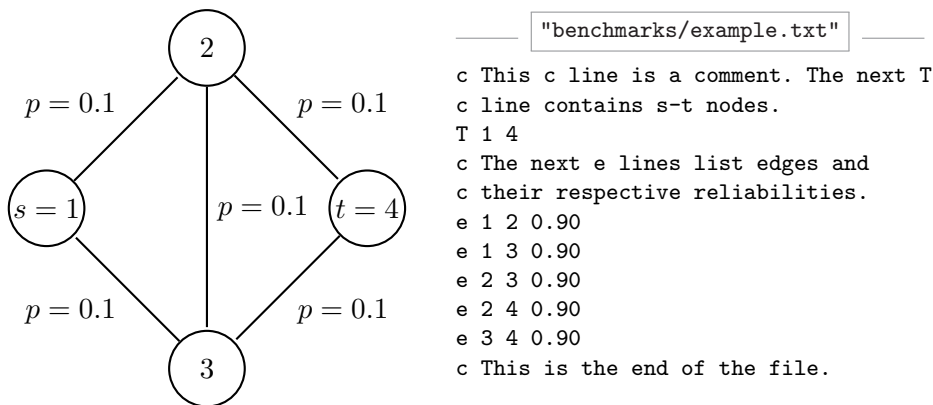


Figure 1: Left: An example instance of the *source-terminal* network reliability problem. Right: Associated input format as shown in the contents of the file “example.txt”.

To showcase computations for the *source-terminal* network reliability problem, we describe next the file format to represent an instance of the problem. As an example, the file located in “benchmarks/example.txt” contains a description of the instance shown in Fig. 1. In particular, every line is interpreted as follows:

- Lines starting with a “c” character contain comments that are ignored when parsing the input into computer programs.
- A line starting with a “T” character contains the set of terminals. In this case it contains nodes s and t in V . Thus, the “T” character is followed by s and t node indices.
- Lines starting with an “e” character contain edge information. Thus, for an edge $(i, j) = e \in E$ such that $i, j \in V$, the character “e” is followed by node indices i and j as well as its respective reliability $1 - p_e$.

The set of benchmarks contained in the folder “benchmarks” uses the instance format just described. In the following section we describe these benchmarks in detail.

2 The Square Grid Benchmarks

We consider square grid networks of size $N \times N$. While there are numerous benchmark possibilities, grids do offer the following advantages:

- For $N > 2$ they cannot be reduced using parallel-series techniques.
- Their size can be arbitrarily increased until rendering exact methods impractical.
- Element failure probabilities can be varied to challenge simulation methods in the rare-event regime.

In this document we consider uniform edge failure probabilities p and let the source-terminal nodes be a pair of nodes located at opposite corners of the $N \times N$ square grid (e.g. Fig. 2). Also, we consider various values of the size parameter N and various values for the failure probability p . In particular, we consider:

- $N = 3, 4, 5, 6, 7, 8, 9, 10, 20, 30, \dots, 100$.
- 5 cases of the failure probability $p = 1 \times 10^{-p_r}$, where p_r is the rarity parameter and we let $p_r = 1, 2, 3, 4, 5$.

The folder “**benchmarks**” contains subfolders “**benchmarks/p{ p_r }**”, and each subfolder contains input instances “**benchmarks/p{ p_r }/grid{ N }.txt**”. For example, the grid network of size 100×100 and edge failure probabilities of $p = 1 \times 10^{-5}$ is located in “**benchmarks/p5/grid100.txt**”.

As a reference, we provide preliminary reliability estimates for this set of benchmarks using crude Monte Carlo simulation (CMC) as well as methods that have been popularized in the Civil Engineering community. More specifically, we use the State Space Partition (SSP) method [1], a generalization of the Selective Recursive Decomposition [3], to estimate theoretical bounds on the failure probability of networks.

We used a high-performance cluster to run numerical experiments in parallel. Each node of the cluster had a 12-core 2.83 GHz processor, with 48GB of main memory (4GB each core), and each experiment was run on a single core. Each experiment consisted of running a method (CMC or SSP) on a given benchmark. The timeout for each experiment was set to 7.8 hours.

The following section discusses experiment results, while highlighting main trends and observations.

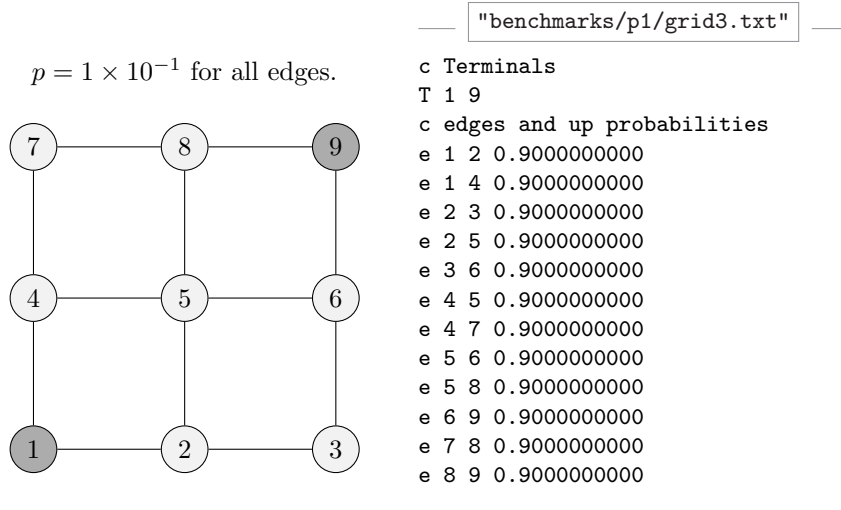


Figure 2: Grid Network of size 3×3 (i.e. $N = 3$). Source and terminal nodes are the ones shaded at the corners.

3 Numerical Experiments

We provide tabulated results summarizing the experiment outcomes. For Crude Monte Carlo simulation (CMC) we display the unreliability estimate $\hat{u}_{s,t}$, sample variance $\hat{\sigma}^2$, the number of sample draws N_s we obtained within the timeout threshold of 7.8 hours, and the estimator coefficient of variation CoV. Tables 1-5 summarize results for all cases of the size parameter N and edge failure probabilities p . It is easy to see that, as the failure probability becomes smaller, the estimators become less reliable. For example, we can use our knowledge of the exact coefficient of variation squared for Bernoulli trials and realize that $\sigma^2/\mu^2 = 1/u_{s,t} - 1$. Thus, the smaller the exact failure probability $u_{s,t}$, the greater the error in CMC experiments.

In practice, for a finite yet large sample size N_s , the central limit theorem is assumed valid such that confidence intervals can be obtained from the sample mean $\hat{u}_{s,t}$ and the sample variance $\hat{\sigma}^2$. For example, $\hat{u}_{s,t} \pm 1.96 \cdot \hat{\sigma}/\sqrt{N_s}$ would give the widely used 95% confidence intervals. Clearly, CMC is going to be challenged by small values of $u_{s,t}$ and its rate of convergence. Thus, when possible, a more reliable approach consists of computing bounds on $u_{s,t}$ with 100% confidence.

For the theoretical method, namely the State Space Partition (SSP) method, we display lower and upper bounds, denoted " $\leq u_{s,t}$ " and " $\geq u_{s,t}$ ", respectively. Also, we show the runtime in seconds. Tables 6-10 summarize

Table 1: CMC estimates for $p = 1 \times 10^{-1}$.

| N | $\hat{u}_{s,t}$ | $\hat{\sigma}^2$ | N_s | CoV | Time [s] |
|-----|-----------------|------------------|-----------|----------|----------|
| 3 | 0.027495 | 0.026739 | 360528500 | 0.000313 | 28080.00 |
| 4 | 0.024968 | 0.024344 | 230806400 | 0.000411 | 28080.00 |
| 5 | 0.024433 | 0.023836 | 159286900 | 0.000501 | 28080.00 |
| 6 | 0.024349 | 0.023756 | 116834700 | 0.000586 | 28080.00 |
| 7 | 0.024302 | 0.023711 | 88625840 | 0.000673 | 28080.00 |
| 8 | 0.024346 | 0.023754 | 68984150 | 0.000762 | 28080.00 |
| 9 | 0.024350 | 0.023757 | 46792120 | 0.000925 | 28080.00 |
| 10 | 0.024367 | 0.023773 | 43924870 | 0.000955 | 28080.00 |
| 20 | 0.024321 | 0.023729 | 11250640 | 0.001888 | 28080.00 |
| 30 | 0.024316 | 0.023725 | 4986994 | 0.002837 | 28080.00 |
| 40 | 0.024276 | 0.023687 | 2758273 | 0.003817 | 28080.00 |
| 50 | 0.024197 | 0.023611 | 1636627 | 0.004964 | 28080.00 |
| 60 | 0.024277 | 0.023688 | 1110440 | 0.006016 | 28080.02 |
| 70 | 0.024292 | 0.023702 | 777959 | 0.007185 | 28080.00 |
| 80 | 0.024197 | 0.023612 | 605777 | 0.008159 | 28080.02 |
| 90 | 0.024524 | 0.023923 | 468106 | 0.009218 | 28080.03 |
| 100 | 0.024625 | 0.024019 | 375264 | 0.010274 | 28080.00 |

results for all benchmark cases. These bounds refer to the “best bounds” as defined in Paredes and Duenas-Osorio [1]. Clearly, the size parameter N is the most sensitive since bounds tend to be wider as N increases. Also, when bounds converge the failure probability has no effect. However, when the bounds do not converge, both the size and rarity of failure probabilities have an effect on how tight the resulting bounds are. More specifically, for smaller failure probabilities bounds tend to be tighter. Also, we highlight that best bounds obtained by the method introduced in Paredes and Duenas-Osorio [1] give consistently practical lower bounds, even for $N = 100$. Nevertheless, the upper bound becomes unpractical as the size parameter increases.

For convenience, results in Tables 1-10 are saved in readable text using the comma separated values (CSV) format. For example, for a fixed value of $p_r = 1$, tabulated results for CMC as in Table 1 can be found under “logs/log_cmc_p1.txt”.

4 Concluding Remarks

Network reliability estimation continues to be untractable in practice, as exact methods and simulation methods remain challenged by both the size

Table 2: CMC estimates for $p = 1 \times 10^{-2}$.

| N | $\hat{u}_{s,t}$ | $\hat{\sigma}^2$ | N_s | CoV | Time [s] |
|-----|-----------------|------------------|-----------|----------|----------|
| 3 | 0.000207 | 0.000207 | 385711900 | 0.003539 | 28080.00 |
| 4 | 0.000204 | 0.000204 | 249361400 | 0.004430 | 28080.00 |
| 5 | 0.000204 | 0.000204 | 170186400 | 0.005369 | 28080.00 |
| 6 | 0.000206 | 0.000206 | 124414700 | 0.006248 | 28080.00 |
| 7 | 0.000204 | 0.000204 | 92643560 | 0.007281 | 28080.00 |
| 8 | 0.000206 | 0.000206 | 73038950 | 0.008143 | 28080.00 |
| 9 | 0.000200 | 0.000200 | 58639050 | 0.009229 | 28080.00 |
| 10 | 0.000204 | 0.000204 | 39187910 | 0.011174 | 28080.00 |
| 20 | 0.000211 | 0.000211 | 10122320 | 0.021655 | 28080.00 |
| 30 | 0.000201 | 0.000201 | 4397413 | 0.033592 | 28080.00 |
| 40 | 0.000198 | 0.000198 | 2325853 | 0.046621 | 28080.00 |
| 50 | 0.000207 | 0.000207 | 1538490 | 0.056071 | 28080.01 |
| 60 | 0.000205 | 0.000205 | 1016046 | 0.069330 | 28080.02 |
| 70 | 0.000202 | 0.000201 | 729454 | 0.082470 | 28080.02 |
| 80 | 0.000201 | 0.000201 | 562967 | 0.094063 | 28080.04 |
| 90 | 0.000196 | 0.000196 | 432778 | 0.108455 | 28080.04 |
| 100 | 0.000168 | 0.000168 | 445975 | 0.115460 | 28080.02 |

Table 3: CMC estimates for $p = 1 \times 10^{-3}$.

| N | $\hat{u}_{s,t}$ | $\hat{\sigma}^2$ | N_s | CoV | Time [s] |
|-----|-----------------|------------------|-----------|----------|----------|
| 3 | 1.992048e-06 | 1.992044e-06 | 394066800 | 0.035691 | 28080.00 |
| 4 | 2.161132e-06 | 2.161127e-06 | 254033500 | 0.042679 | 28080.00 |
| 5 | 1.972440e-06 | 1.972436e-06 | 170347400 | 0.054554 | 28080.00 |
| 6 | 1.747683e-06 | 1.747680e-06 | 125880900 | 0.067420 | 28080.00 |
| 7 | 1.971131e-06 | 1.971127e-06 | 95376730 | 0.072932 | 28080.00 |
| 8 | 2.041193e-06 | 2.041189e-06 | 74956150 | 0.080845 | 28080.00 |
| 9 | 1.868513e-06 | 1.868510e-06 | 58870340 | 0.095346 | 28080.00 |
| 10 | 1.718392e-06 | 1.718389e-06 | 47719040 | 0.110431 | 28080.00 |
| 20 | 2.070359e-06 | 2.070355e-06 | 12075200 | 0.200000 | 28080.00 |
| 30 | 1.483843e-06 | 1.483841e-06 | 5391407 | 0.353553 | 28080.00 |
| 40 | 1.808447e-06 | 1.808444e-06 | 2764803 | 0.447213 | 28080.00 |
| 50 | 1.111608e-06 | 1.111608e-06 | 1799195 | 0.707107 | 28080.00 |
| 60 | 8.220730e-07 | 8.220730e-07 | 1216437 | 1.000000 | 28080.00 |
| 70 | 0.000000e+00 | 0.000000e+00 | 865940 | NaN | 28080.02 |
| 80 | 3.030152e-06 | 3.030147e-06 | 660033 | 0.707106 | 28080.03 |
| 90 | 1.916770e-06 | 1.916770e-06 | 521711 | 1.000000 | 28080.04 |
| 100 | 0.000000e+00 | 0.000000e+00 | 454785 | NaN | 28080.02 |

Table 4: CMC estimates for $p = 1 \times 10^{-4}$.

| N | $\hat{u}_{s,t}$ | $\hat{\sigma}^2$ | N_s | CoV | Time [s] |
|-----|-----------------|------------------|-----------|----------|----------|
| 3 | 7.655205e-09 | 7.655205e-09 | 391890200 | 0.577350 | 28080.00 |
| 4 | 2.379872e-08 | 2.379872e-08 | 252114400 | 0.408248 | 28080.00 |
| 5 | 1.161015e-08 | 1.161015e-08 | 172263100 | 0.707107 | 28080.00 |
| 6 | 2.349814e-08 | 2.349814e-08 | 127669700 | 0.577350 | 28080.00 |
| 7 | 3.818167e-08 | 3.818167e-08 | 78571740 | 0.577350 | 28080.00 |
| 8 | 3.222889e-08 | 3.222889e-08 | 62056120 | 0.707107 | 28080.00 |
| 9 | 0.000000e+00 | 0.000000e+00 | 49193670 | NaN | 28080.00 |
| 10 | 0.000000e+00 | 0.000000e+00 | 41207310 | NaN | 28080.00 |
| 20 | 0.000000e+00 | 0.000000e+00 | 9946345 | NaN | 28080.00 |
| 30 | 0.000000e+00 | 0.000000e+00 | 4459871 | NaN | 28080.00 |
| 40 | 0.000000e+00 | 0.000000e+00 | 2431569 | NaN | 28080.00 |
| 50 | 0.000000e+00 | 0.000000e+00 | 1531661 | NaN | 28080.00 |
| 60 | 0.000000e+00 | 0.000000e+00 | 1014298 | NaN | 28080.02 |
| 70 | 0.000000e+00 | 0.000000e+00 | 751584 | NaN | 28080.02 |
| 80 | 0.000000e+00 | 0.000000e+00 | 558672 | NaN | 28080.03 |
| 90 | 0.000000e+00 | 0.000000e+00 | 448258 | NaN | 28080.02 |
| 100 | 0.000000e+00 | 0.000000e+00 | 358041 | NaN | 28080.06 |

Table 5: CMC estimates for $p = 1 \times 10^{-5}$.

| N | $\hat{u}_{s,t}$ | $\hat{\sigma}^2$ | N_s | CoV | Time [s] |
|-----|-----------------|------------------|-----------|-----|----------|
| 3 | 0.000000e+00 | 0.000000e+00 | 322488500 | NaN | 28080.00 |
| 4 | 0.000000e+00 | 0.000000e+00 | 212580500 | NaN | 28080.00 |
| 5 | 0.000000e+00 | 0.000000e+00 | 144023700 | NaN | 28080.00 |
| 6 | 0.000000e+00 | 0.000000e+00 | 103975100 | NaN | 28080.00 |
| 7 | 0.000000e+00 | 0.000000e+00 | 78667840 | NaN | 28080.00 |
| 8 | 0.000000e+00 | 0.000000e+00 | 62030430 | NaN | 28080.00 |
| 9 | 1.966564e-08 | 1.966564e-08 | 50850120 | 1.0 | 28080.00 |
| 10 | 0.000000e+00 | 0.000000e+00 | 40639410 | NaN | 28080.00 |
| 20 | 0.000000e+00 | 0.000000e+00 | 10186810 | NaN | 28080.00 |
| 30 | 0.000000e+00 | 0.000000e+00 | 4435675 | NaN | 28080.00 |
| 40 | 0.000000e+00 | 0.000000e+00 | 2499222 | NaN | 28080.00 |
| 50 | 0.000000e+00 | 0.000000e+00 | 1533004 | NaN | 28080.00 |
| 60 | 0.000000e+00 | 0.000000e+00 | 1045440 | NaN | 28080.00 |
| 70 | 0.000000e+00 | 0.000000e+00 | 757264 | NaN | 28080.03 |
| 80 | 0.000000e+00 | 0.000000e+00 | 572322 | NaN | 28080.00 |
| 90 | 0.000000e+00 | 0.000000e+00 | 446586 | NaN | 28080.02 |
| 100 | 0.000000e+00 | 0.000000e+00 | 363252 | NaN | 28080.02 |

Table 6: SSP estimates for $p = 1 \times 10^{-1}$.

| N | $\leq u_{s,t}$ | $\geq u_{s,t}$ | Time [s] |
|-----|------------------|------------------|----------|
| 3 | 2.7497828593e-02 | 2.7497828593e-02 | 1.22 |
| 4 | 2.4953650423e-02 | 2.4953650423e-02 | 206.49 |
| 5 | 2.4443410495e-02 | 2.4443410495e-02 | 17845.83 |
| 6 | 2.4326683271e-02 | 1.1545304605e-01 | 28080.25 |
| 7 | 2.4320145065e-02 | 1.1814674212e-01 | 28080.08 |
| 8 | 2.4282119282e-02 | 1.1980542156e-01 | 28080.79 |
| 9 | 2.4331994910e-02 | 1.1980542156e-01 | 28081.26 |
| 10 | 2.4319970641e-02 | 5.5228597094e-01 | 28081.17 |
| 20 | 2.4285225883e-02 | 9.9127294031e-01 | 28080.32 |
| 30 | 2.4287575021e-02 | 9.9900193336e-01 | 28080.89 |
| 40 | 2.4282064396e-02 | 1.0000000000e+00 | 28080.47 |
| 50 | 2.4282063212e-02 | 1.0000000000e+00 | 28080.28 |
| 60 | 2.4282050156e-02 | 1.0000000000e+00 | 28080.35 |
| 70 | 2.4281864714e-02 | 1.0000000000e+00 | 28080.25 |
| 80 | 2.4280866453e-02 | 1.0000000000e+00 | 28080.18 |
| 90 | 2.4275485956e-02 | 1.0000000000e+00 | 28080.38 |
| 100 | 2.4241322212e-02 | 1.0000000000e+00 | 28080.12 |

Table 7: SSP estimates for $p = 1 \times 10^{-2}$.

| N | $\leq u_{s,t}$ | $\geq u_{s,t}$ | Time [s] |
|-----|------------------|------------------|----------|
| 3 | 2.0798597679e-04 | 2.0798597679e-04 | 1.20 |
| 4 | 2.0409116253e-04 | 2.0409116253e-04 | 203.02 |
| 5 | 2.0403122638e-04 | 2.0403122638e-04 | 17859.22 |
| 6 | 2.0403040483e-04 | 2.4201074932e-04 | 28080.19 |
| 7 | 2.0403039597e-04 | 2.3221412260e-04 | 28080.17 |
| 8 | 2.0403034040e-04 | 2.0185072696e-04 | 28080.68 |
| 9 | 2.0403039799e-04 | 2.0858740071e-04 | 28081.37 |
| 10 | 2.0403034040e-04 | 5.4793964334e-03 | 28080.60 |
| 20 | 2.0402897438e-04 | 1.3480095400e-01 | 28081.16 |
| 30 | 2.0402897438e-04 | 3.3460268034e-01 | 28080.85 |
| 40 | 2.0397898055e-04 | 7.2035636932e-01 | 28080.42 |
| 50 | 2.0397898055e-04 | 8.5661128560e-01 | 28080.33 |
| 60 | 2.0397898055e-04 | 9.2669213096e-01 | 28080.28 |
| 70 | 2.0397898055e-04 | 9.5336259770e-01 | 28080.17 |
| 80 | 2.0397898055e-04 | 9.7032996155e-01 | 28080.40 |
| 90 | 2.0397898055e-04 | 9.8112435217e-01 | 28080.17 |
| 100 | 2.0397898055e-04 | 9.8799158681e-01 | 28081.19 |

Table 8: SSP estimates for $p = 1 \times 10^{-3}$.

| N | $\leq u_{s,t}$ | $\geq u_{s,t}$ | Time [s] |
|-----|------------------|------------------|----------|
| 3 | 2.0079989600e-06 | 2.0079989600e-06 | 1.25 |
| 4 | 2.0040090120e-06 | 2.0040090120e-06 | 204.14 |
| 5 | 2.0040030120e-06 | 2.0040030120e-06 | 17772.96 |
| 6 | 2.0040079128e-06 | 2.0071351646e-06 | 28080.17 |
| 7 | 2.0040030040e-06 | 2.0071355646e-06 | 28080.15 |
| 8 | 2.0040030039e-06 | 4.6752864837e-06 | 28080.89 |
| 9 | 2.0040030039e-06 | 2.3251507015e-06 | 28080.54 |
| 10 | 2.0040030039e-06 | 8.7338433202e-06 | 28080.65 |
| 20 | 2.0040029900e-06 | 2.0816183241e-03 | 28081.00 |
| 30 | 2.0040029900e-06 | 6.7570300814e-03 | 28080.75 |
| 40 | 2.0039979900e-06 | 1.3041116971e-01 | 28080.46 |
| 50 | 2.0039979900e-06 | 1.8633581325e-01 | 28080.29 |
| 60 | 2.0039979900e-06 | 2.2904871125e-01 | 28080.25 |
| 70 | 2.0039979900e-06 | 2.6298910334e-01 | 28080.32 |
| 80 | 2.0039979900e-06 | 2.9543530217e-01 | 28080.22 |
| 90 | 2.0039979900e-06 | 3.2645308817e-01 | 28080.46 |
| 100 | 2.0039979900e-06 | 3.5610534585e-01 | 28080.15 |

Table 9: SSP estimates for $p = 1 \times 10^{-4}$.

| N | $\leq u_{s,t}$ | $\geq u_{s,t}$ | Time [s] |
|-----|------------------|------------------|----------|
| 3 | 2.0007999900e-08 | 2.0007999900e-08 | 1.25 |
| 4 | 2.0004000900e-08 | 2.0004000900e-08 | 202.35 |
| 5 | 2.0004000300e-08 | 2.0004000300e-08 | 17818.31 |
| 6 | 2.0004000300e-08 | 2.0004433478e-08 | 28080.18 |
| 7 | 2.0004000300e-08 | 2.0004315610e-08 | 28080.15 |
| 8 | 2.0004000300e-08 | 2.2630750518e-08 | 28080.68 |
| 9 | 2.0004000300e-08 | 2.0004000661e-08 | 28081.42 |
| 10 | 2.0004000300e-08 | 2.0354197423e-08 | 28081.19 |
| 20 | 2.0004000300e-08 | 3.0486183852e-05 | 28080.32 |
| 30 | 2.0004000300e-08 | 7.2809834903e-05 | 28080.84 |
| 40 | 2.0003999800e-08 | 1.3988733361e-02 | 28080.44 |
| 50 | 2.0003999800e-08 | 2.0479851949e-02 | 28080.31 |
| 60 | 2.0003999800e-08 | 2.5666177110e-02 | 28080.51 |
| 70 | 2.0003999800e-08 | 3.0041047220e-02 | 28080.15 |
| 80 | 2.0003999800e-08 | 3.4396273663e-02 | 28080.14 |
| 90 | 2.0003999800e-08 | 3.8731944642e-02 | 28080.82 |
| 100 | 2.0003999800e-08 | 4.3048147964e-02 | 28080.10 |

Table 10: SSP estimates for $p = 1 \times 10^{-5}$.

| N | $\leq u_{s,t}$ | $\geq u_{s,t}$ | Time [s] |
|-----|------------------|------------------|----------|
| 3 | 2.0000799999e-10 | 2.0000799999e-10 | 1.22 |
| 4 | 2.0000400009e-10 | 2.0000400009e-10 | 204.98 |
| 5 | 2.0000400003e-10 | 2.0000408862e-10 | 17795.58 |
| 6 | 2.0000400003e-10 | 2.0000406367e-10 | 28080.17 |
| 7 | 2.0000400003e-10 | 2.0000383927e-10 | 28080.14 |
| 8 | 2.0000400003e-10 | 2.0268150995e-10 | 28080.74 |
| 9 | 2.0000400003e-10 | 2.0000402850e-10 | 28081.38 |
| 10 | 2.0000400003e-10 | 2.0042762846e-10 | 28081.18 |
| 20 | 2.0000400003e-10 | 3.0633573682e-07 | 28080.26 |
| 30 | 2.0000400003e-10 | 7.3358723053e-07 | 28080.69 |
| 40 | 2.0000399998e-10 | 1.4088817258e-03 | 28080.43 |
| 50 | 2.0000399998e-10 | 2.0677842896e-03 | 28080.33 |
| 60 | 2.0000399998e-10 | 2.5966358937e-03 | 28080.21 |
| 70 | 2.0000399998e-10 | 3.0453686788e-03 | 28080.18 |
| 80 | 2.0000399998e-10 | 3.4938995785e-03 | 28080.31 |
| 90 | 2.0000399998e-10 | 3.9422286838e-03 | 28082.31 |
| 100 | 2.0000399998e-10 | 4.3903560853e-03 | 28081.76 |

of problem instances and the rarity of system failures, respectively. Perhaps a case-by-case approach will yield the best results in practice.

The present document is subject to changes to better reflect ongoing efforts on system reliability estimation by the SISSRA research group.

5 Acknowledgements

The input file format is adopted from related work by Professor Radislav Vaisman¹. Also, we implement reliability estimation algorithms in Python leveraging the network analysis module NetworkX [4]. Furthermore, in regards to computational resources used in our numerical experiments, we thank the Data Analysis and Visualization Cyberinfrastructure funded by NSF under grant OCI-0959097 and Rice University. Finally, the authors gratefully acknowledge the support by the U.S. National Science Foundation (Grants CMMI-1436845 and CMMI-1541033).

¹<https://people.smp.uq.edu.au/RadislavVaisman/>

References

- [1] Roger Paredes, Leonardo Duenas-Osorio, and Isaac Hernandez-Fajardo. Decomposition Algorithms for Estimating Reliability in Interdependent Lifeline Systems. *Earthquake Engineering & Structural Dynamics (submitted)*, 2018.
- [2] Roger Paredes, Leonardo Dueñas-Osorio, Kuldeep S. Meel, and Moshe Y. Vardi. Network Reliability Estimation in Theory and Practice. *To be submitted to: Reliability Engineering & System Safety*, 2018.
- [3] Hyun-woo Lim and Junho Song. Efficient risk assessment of lifeline networks under spatially correlated ground motions using selective recursive decomposition algorithm. *Earthquake Engineering & Structural Dynamics*, 41(13):1861–1882, oct 2012.
- [4] Daniel A. Schult. Exploring network structure, dynamics, and function using networkx. In *In Proceedings of the 7th Python in Science Conference (SciPy)*, pages 11–15, 2008.